Voltage and Ca^{2+} Dependence of Pre–Steady-State Currents of the Na-Ca Exchanger Generated by Ca^{2+} Concentration Jumps

Michael Kappl, Georg Nagel, and Klaus Hartung
Max-Planck-Institut für Biophysik, D-60596 Frankfurt, Germany

ABSTRACT The Ca^{2+} concentration and voltage dependence of the relaxation kinetics of the Na-Ca exchanger after a Ca^{2+} concentration jump was measured in excised giant membrane patches from guinea pig heart. Ca^{2+} concentration jumps on the cytoplasmic side were achieved by laser flash-induced photolysis of DM-nitrophen. In the Ca-Ca exchange mode a transient inward current is generated. The amplitude and the decay rate of the current saturate at concentrations >10 μM. The integrated current signal, i.e., the charge moved is fairly independent of the amount of Ca^{2+} released. The amount of charge translocated increases at negative membrane potentials, whereas the decay rate constant shows no voltage dependence. It is suggested that Ca^{2+} translocation occurs in at least four steps: intra- and extracellular Ca^{2+} binding and two intramolecular transport steps. Saturation of the amplitude and of the relaxation of the currrent can be explained if the charge translocating reaction step is preceded by two nonelectrogenic steps: Ca^{2+} binding and one conformational transition. Charge translocation in this mode is assigned to one additional conformational change which determines the equilibrium distribution of states. In the Na-Ca exchange mode, the stationary inward current depends on the cytoplasmic Ca^{2+} concentration and voltage. The K_m for Ca^{2+} is 4 μM for guinea pig and 10 μM for rat myocytes. The amplitude of the pre–steady-state current and its relaxation saturate with increasing Ca^{2+} concentrations. In this mode the relaxation is voltage dependent.

INTRODUCTION

The Na-Ca exchanger in heart cells couples the countertransport of three Na^+ ions against one Ca^{2+} ion across the plasma membrane. It is a major transport protein involved in intracellular Ca^{2+} homeostasis (Blaustein and Lederer, 1999). Because the transport stoichiometry is 3 Na^+/1 Ca^{2+}, the activity of the transporter can be monitored by current measurements (Kimura et al., 1986; Mechmann and Pott, 1986; Hilgemann 1989, 1990). Other transport modes observed under appropriate conditions are Na-Na (DiPolo and Beaugé, 1987) and Ca-Ca exchange (Blaustein and Russell, 1975; Bartschat and Lindenmayer, 1980; Slaughter et al., 1983). These self-exchange modes are electroneutral in the steady-state but electrogenic under nonstationary conditions (Hilgemann et al., 1991; Hilgemann, 1996; Kappl and Hartung, 1996b; He et al., 1998).

Recently, relaxation experiments, i.e., voltage and Ca^{2+} concentration steps performed on "giant" excised membrane patches (Hilgemann, 1989), have shown that some of the reaction steps involved in the translocation of Na^+ and Ca^{2+} are very fast with relaxation rate constants of $\sim$5000 s^{-1} or more at 35°C (Hilgemann, 1996; Kappl and Hartung, 1996a, b). Ca^{2+} concentration jumps performed on the cytoplasmic side of the membrane with the photolabile Ca^{2+} chelator 1-(2-nitro-4,5 dimethoxyphenyl)-*N*,*N*,*N*′,*N*′,-tetrakis [(oxycarbonyl)methyl]-1,2-ethandiamine (DM)-nitrophen elicit a transient inward charge translocation (pre–steady-state current) by the Na-Ca-exchanger in the Na-Ca exchange mode and the Ca-Ca exchange mode (Kappl and Hartung, 1996a, b). A number of control experiments have shown that the transient current is related to the Na-Ca exchanger (Kappl and Hartung 1996b); it is not observed if the external solution contains no substrate (Na^+ or Ca^{2+}), it is not observed if the external solution contains Ni^+ in addition to Na^+ to inhibit the exchanger, the transient current increases if the cytoplasmic side of the membrane is treated with chymotrypsin which removes inactivation (Hilgemann, 1990).

The transient current decays to a stationary current in the Na-Ca exchange mode and to zero in the Ca-Ca exchange mode. These experiments show: 1) under saturating conditions the rise-time of the pre–steady-state current is <0.1 ms, indicating fast Ca^{2+} binding; 2) Ca^{2+} translocation is electrogenic; 3) the Ca-loaded enzyme translocates negative charge; and 4) in the stationary state Na^+ translocation is rate-limiting for Na-Ca exchange.

We report experiments on the voltage and Ca^{2+} concentration dependence of the pre—steady-state current in the Ca-Ca- and in the Na-Ca exchange mode elicited by a Ca^{2+} concentration jump. It should be noted that under the conditions applied here, Na-Ca exchange always means Na^+ entry/Ca^{2+} exit mode (Blaustein and Lederer, 1999), which is also addressed as inward exchange mode (Matsuoka and Hilgemann, 1992).

The experiments presented here suggest: 1) Ca^{2+} binding to cytoplasmic sites is not electrogenic; 2) intramolecular

Received for publication 13 December 2000 and in final form 14 August 2001.

Address reprint requests to Corresponding author: Dr. K. Hartung, Max-Planck-Institut für Biophysik, D-60596 Frankfurt/Main, Germany. Tel.: 49-69-6303-307; Fax: 49-69-6303-305; E-mail: hartung@mpibp-frankfurt.mpg.de.

M. Kappl's present address: Universität Siegen, Physikalische Chemie, Adolf-Reichwein-Strasse, D-57076 Siegen, Germany.

0006-3495/01/11/2628/11 $2.00

Ca^{2+} translocation occurs in at least two steps; 3) there is at least one nonelectrogenic step intercalated between Ca^{2+} binding and electrogenic Ca^{2+} translocation; and 4) a nonelectrogenic step is rate-limiting.

Material and Methods

Experimental procedures were described in detail previously (Kappl and Hartung, 1996b). In brief: "giant" membrane patches in the inside-out configuration were excised from membrane "blebs" formed by isolated ventricular myocytes from guinea pig as described by Hilgemann (1989). In a few experiments cells from rat heart were used. Patch pipettes had openings between 15 and 22 μm. If not indicated otherwise, membrane patches were treated with α-chymotrypsin (1 min, 1 mg/ml) to remove regulatory mechanisms of the exchanger (Hilgemann, 1990). Ca^{2+} concentration jumps were performed using the photolabile Ca^{2+} chelator DM-nitrophen (Kaplan and Ellis-Davies, 1988). To measure currents in the Ca-Ca exchange mode, the patch pipette was filled with (in mM): 5 Ca^{2+}, 100 Li^{+}, 20 Cs^{+}, 20 TEA, 0.02 verapamil, 10 HEPES. In the Na-Ca exchange mode the pipette contained 100 mM Na^{+} instead of Li^{+} and also 10 mM EGTA and 2 mM Mg^{2+}. If not indicated otherwise, the bath (cytoplasmic solution) for photolytic Ca^{2+} concentration jumps contained (in mM): 0.45 DM-nitrophen (Calbiochem, Bad Soden, Germany), 0.44 Ca^{2+},100 Li^{+}, 20 Cs^{+}, 20 tetraethylammonium, 10 HEPES. The free Ca^{2+} concentration under these conditions is ~0.2 μM. All solutions were adjusted to pH 7.1. Unless mentioned otherwise, experiments were performed at 25°C.

The magnitude of the Ca^{2+} concentration jump was adjusted by changing the intensity of the laser flash with calibrated neutral density filters (Melles and Griot, Bensheim, Germany). Stationary exchange currents were also activated by Ca^{2+}-containing solutions on the cytoplasmic side. Such experiments were also used to calibrate the amount of Ca^{2+} released from DM-nitrophen (Kappl and Hartung, 1996b). The time course of Ca^{2+} release after a flash and rebinding to unphotolyzed DM-nitrophen (Zucker, 1993) was calculated by solving a set of simultaneous differential equations published by Ellis-Davies et al. (1996). These simulations (Fig. 1) show that, with the concentrations of Ca^{2+} and DM-nitrophen used here, the photolysis of DM-nitrophen approximates a step function if at least 10% DM-nitrophen are photolyzed, i.e., the initial overshoot is ~17% larger than the stationary value and decays to the stationary state with $\tau = 0.7$ ms. At lower fractions of DM-nitrophen photolyzed a Ca^{2+} spike is generated; e.g., at 1% photolysis the peak Ca^{2+} concentration is 10 times larger than the stationary value and decays with $\tau = 1.5$ ms. It should be noted that the Ca^{2+} concentrations indicated in the text refer to the stationary state.

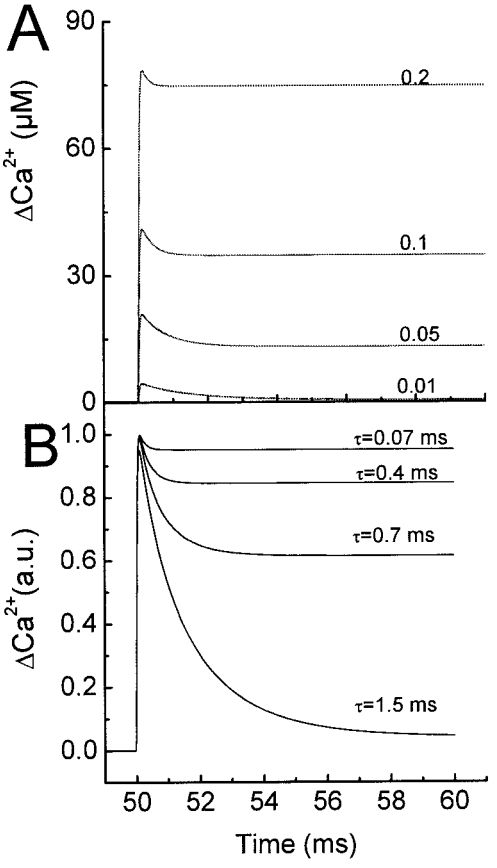

FIGURE 1 Simulation of the time course of the free Ca^{2+} concentration after the photolysis of different fractions (0.01, 0.05, 0.1, and 0.2) of total DM-nitrophen (0.47 mM). The total concentration of Ca^{2+} was 0.46 mM. The concentration of free Ca^{2+} was calculated by numeric integration of a set of differential equations. Association and dissociation constants (8×10^7 $M^{-1}s^{-1}$ and 0.4 s^{-1}) and the rate of release of Ca^{2+} from bleached DM-nitrophen (38,000 s^{-1}) were taken from Ellis-Davies et al. (1996). Ca^{2+} binding to the photoproducts is assumed to be negligible (K_d = 3 mM). At $t = 50$ ms different fractions of DM-nitrophen were photolyzed using the pulse function of the Scientist software. (*A*) Time course of the free Ca^{2+} concentration after photolysis of 1, 5, 10, or 20% of total DM-nitrophen at $t = 50$ ms. The peak and plateau concentrations were 78 vs. 75, 41 vs. 35, 21 vs. 13, and 4.4 vs. 0.45 μM. The time course of the Ca^{2+} signal can be fitted by a sum of two exponential functions and a constant. The decay time constant is indicated in *B*. (*B*) Normalized time course of the Ca^{2+} signals shown in *A*.

Currents were measured by an Axopatch 200 A amplifier (Axon Instruments, Foster City, CA) in the capacitive feedback mode. To eliminate the artifact generated by the discharge of the laser, the reset function of the amplifier (lasting 50 μs) discharging the feedback capacitor of the amplifier was activated 22 μs before the laser flash was triggered (Kappl and Hartung, 1996b). The recording bandwidth was set to 5 or 10 kHz, depending on the magnitude of the current signal and the time course of the signal. Current records were fitted to a sum of two exponential functions using the routine provided by the pClamp package (Axon Instruments). Scientist software (MicroMath Scien-

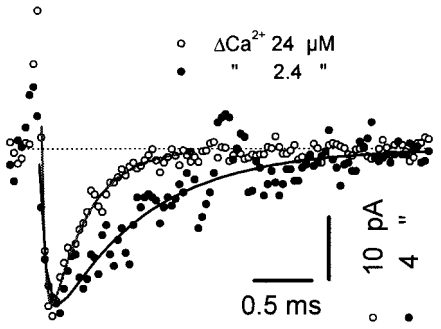

FIGURE 2 Current signals in the Ca-Ca exchange mode after Ca^{2+} concentration jumps of different magnitude generated on the cytoplasmic side of the membrane. The signal obtained at 2.4 μM was scaled up with a factor of 2.5. The continuous lines are biexponential fits with time constants $\tau_1 = 0.034$, 0.06 and $\tau_2 = 0.32$, 0.8 ms for $\Delta Ca^{2+} = 24$ μM and $\Delta Ca^{2+} = 2.4$ μM, respectively. The dotted line indicates the zero current level.

tific Software, Salt Lake City, UT) was used to fit a system of simultaneous differential equations to currents records obtained after a Ca^{2+} concentration jump (Fig. 13) and to perform simulations with reaction model suggested for Ca^{2+} translocation (see Appendix).

Time constants obtained in the Ca-Ca exchange mode are denoted $\tau_{i,Ca\text{-}Ca}$ and those obtained in the Na-Ca exchange mode are given as $\tau_{i;Na\text{-}Ca}$.

RESULTS

Ca-Ca exchange

In the absence of extra- and intracellular Na^+, the Na-Ca exchanger performs stationary electroneutral Ca-Ca exchange if Ca^{2+} is available on both sides of the membrane (Blaustein and Russell, 1975; Bartschat and Lindenmayer, 1980). Nevertheless, forcing the exchanger in this mode from one equilibrium distribution of state to another by applying a voltage or Ca^{2+} concentration jump elicits a transient current indicating a redistribution of charge correlated with the establishment of a new equilibrium (Hilgemann, 1996; Kappl and Hartung, 1996a, b). It is assumed that inward and outward movement of Ca^{2+} occurs via the same intermediates (Fig. 12).

Ca^{2+} concentration dependence of the pre–steady-state current in the Ca-Ca exchange mode

The first set of experiments illustrates the effect of the magnitude of a Ca^{2+} concentration jump on the transient current. All experiments were performed with 5 mM extracellular Ca^{2+} at 0 mV membrane potential. The cytoplasmic Ca^{2+} concentration before the concentration jump was 0.1 to 0. 2 μM.

Fig. 2 shows current records obtained with two different Ca^{2+} concentration jumps, $\Delta Ca = 2.4$ μM and $\Delta Ca = 24$ μM which were achieved by adjusting the intensity of the laser flash. For comparison the current records were scaled and superimposed (see figure legend). According to convention, negative current indicates the flow of positive charge from the extracellular to the intracellular side. The time course of the signal can be described by a sum of two exponential functions with rise-time $\tau_{1,Ca\text{-}Ca}$ and decay time $\tau_{2,Ca\text{-}Ca}$.

Although the rise-time cannot be evaluated quantitatively (see Material and Methods and Kappl and Hartung, 1996b) it is important to note that the experiments do not show a significant increment of the rise-time at low Ca^{2+} concentrations i.e., even at the lowest Ca^{2+} concentrations, the time to peak is <0.1 ms. The low correlation between Ca^{2+} released and the time to peak is at least partially attributable to the formation of Ca^{2+} spikes (Figs. 2 and 7).

In contrast, the amplitude of the peak inward current and the decay rate constant $1/\tau_{2,Ca\text{-}Ca}$ are clearly Ca^{2+}-dependent (Figs. 2, 3) and saturate at concentrations >15 μM. As outlined previously, the formation of a Ca^{2+} spike (Fig. 1 and Zucker, 1993) at low fractions of DM-nitrophen photolyzed distorts the Ca^{2+} dependence of all these parameters because the initial Ca^{2+} concentration is higher than indicated on the ordinate and prevents the determination of the apparent Ca^{2+} affinity. It is, however, important to note that these parameters saturate because this provides important information concerning the assignment of electrogenicity to individual reaction steps (see Discussion). Fig. 3 *C* shows the Ca^{2+} dependence of the integrated current signal, i.e., the amount of charge moved after the Ca^{2+} concentration jump. This parameter shows less Ca^{2+} dependence than the relaxation rate constant and the peak current and is virtually constant between 2 and 50 μM. It can be easily shown that in the Ca-Ca exchange mode the amount of charge translocated represents the shift from one equilibrium to another, which is by definition independent from the way by which it is reached. Therefore, this parameter which is determined only by the final Ca^{2+} concentration can be evaluated over the whole concentration range. The low correlation between the amount of Ca^{2+} released and the charge translocated indicates that the equilibrium distribution of states is determined by transitions other than Ca^{+2} binding as long as some Ca^{2+} is available on the cytoplasmic side.

Voltage dependence of the pre–steady-state current in the Ca-Ca exchange mode generated by a Ca^{2+} concentration jump

The voltage dependence of the pre–steady-state current was investigated by applying Ca^{2+} concentration jumps at different membrane potentials. Fig. 4 shows current signals obtained at +75 and −75 mV generated by identical Ca^{2+} concentration jumps. At +75 mV the amplitude is reduced by a factor of 2.15, but the time course is indistinguishable from that at −75 mV as can be deduced from the scaled and

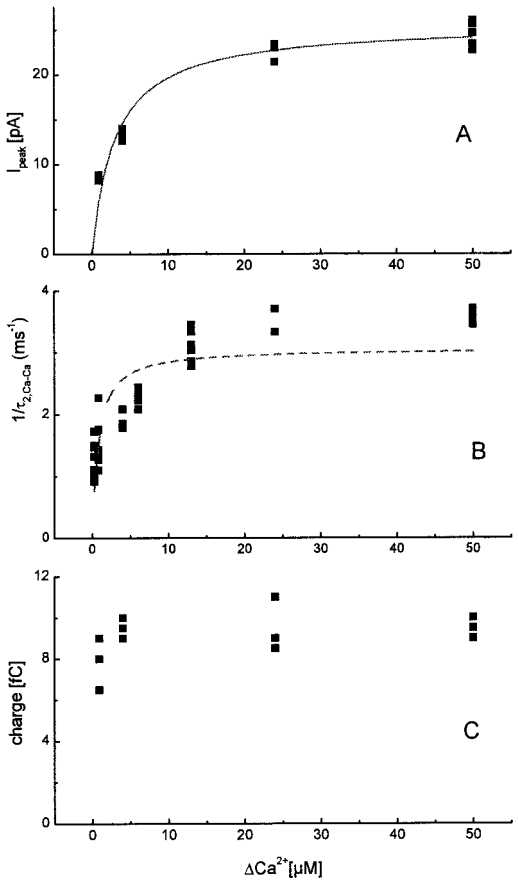

FIGURE 3 (*A*) Ca^{2+} dependence of the maximum of the transient current in the Ca-Ca exchange mode. A hyperbola (Michaelis-Menten kinetics) has been fitted to the data (continuous line). $K_m = 3$ μM. (*B*) Ca^{2+} dependence of the relaxation rate constant of the decay of the transient current. A hyperbolic function is included for comparison. The cytoplasmic concentrations of DM-nitrophen and Ca^{2+} were 470 and 460 μM, respectively. The amount of Ca^{2+} released was adjusted by changing the energy of the laser flash. This leads to a Ca^{2+} spike which distorts the Ca^{2+} dependence at low fractions of DM-nitrophen photolyzed (see Discussion). (*C*) Ca^{2+} dependence of the integrated current signal (charge) generated by Ca^{2+} concentration jumps in the Ca-Ca exchange mode. The charge translocated after a Ca^{2+} concentration jump is correlated with the shift of the equilibrium distribution of states and therefore not affected by Ca^{2+} spikes.

superimposed records. The decay time constant $1/\tau_{2,Ca-Ca}$ is nearly constant between ± 100 mV (Fig. 5 *B*). Fig. 5 *A* shows that between ±100 mV, the amount of charge translocated increases with hyperpolarization. Fitting the data with a Boltzmann distribution (Hilgemann, 1996) yields a maximal charge of ~32 fC, a midpoint V′ of +65 mV and an apparent charge (dielectric coefficient α) of 0.38. From the maximal charge and the apparent charge it is estimated that the patch contains $\sim 5 \times 10^5$ exchanger molecules. Under similar conditions, an apparent charge 0.32 was obtained by voltage jump experiments (Hilgemann, 1996).

Thus, in the Ca-Ca exchange mode the amount of charge translocated after a saturating Ca^{2+} concentration jump

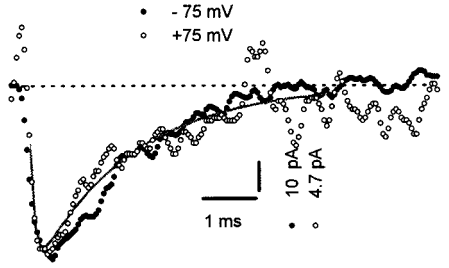

FIGURE 4 Voltage dependence of transient currents generated by Ca^{2+} concentration jumps in the Ca-Ca exchange mode. Ca^{2+} concentration jumps were elicited at −75 and +75 mV holding potential. The current signal measured at +75 mV was scaled by a factor of 2.15. The continuous curve is a biexponential fit with $\tau_1 = 0.05$ ms and $\tau_2 = 1.25$ ms. The dotted line indicates the zero current level.

depends on the membrane potential but is independent (at 0 mV) of the magnitude of the Ca^{2+} concentration jump, whereas the relaxation rate $1/\tau_{2,Ca-Ca}$ is Ca^{2+}-dependent and saturating but not voltage-dependent.

Inward Na-Ca exchange current

Ca^{2+} concentration dependence of the stationary inward current

The Ca^{2+} concentration dependence of the stationary Na-Ca exchange current at 0 mV was determined by perfusion of

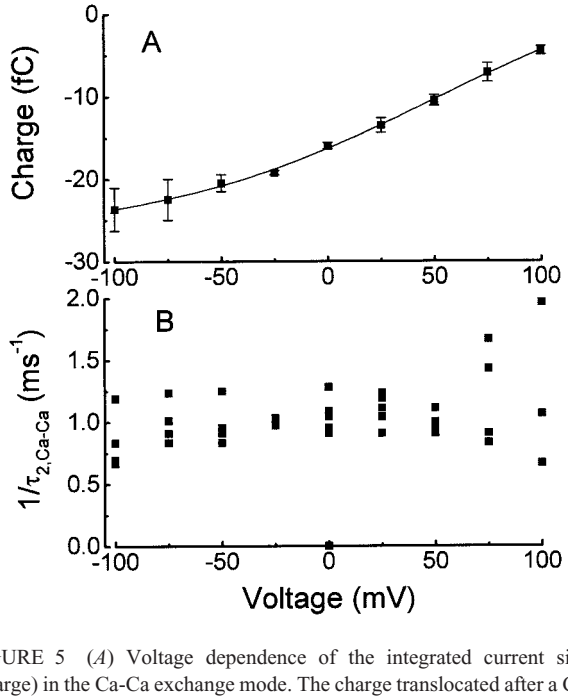

FIGURE 5 (*A*) Voltage dependence of the integrated current signal (charge) in the Ca-Ca exchange mode. The charge translocated after a Ca^{2+} concentration jump increases at negative holding potentials. The continuous line is a fit of the Boltzmann distribution ($Q = Q_{max}(1/(1 + \exp((v - v')/k))$) with $k = \alpha zF/RT$, $\alpha = 0.38$, $Q_{max} = 32$ fC, and $V' = +65$ mV. (*B*) Voltage dependence of the relaxation rate constant of the decay of the transient current, $1/\tau_{2,Ca-Ca}$.

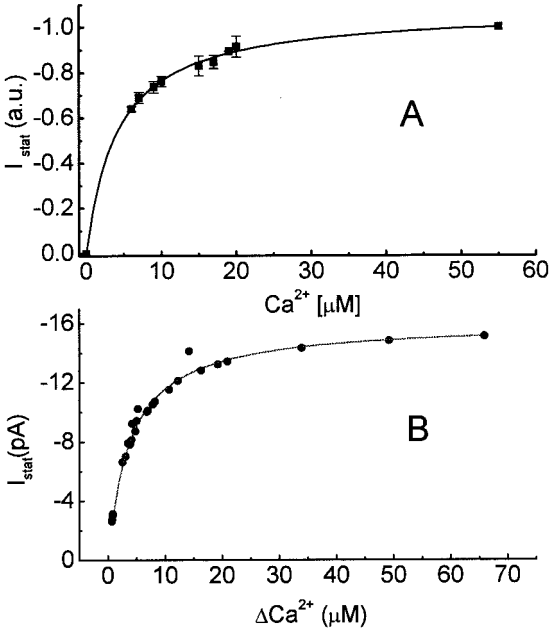

FIGURE 6 (*A*) Ca^{2+} dependence of stationary inward current in the inward Na-Ca exchange mode at 0 mV. Currents were elicited by the stationary application of solutions containing different concentrations of Ca^{2+} on the cytoplasmic side of excised membrane patches. Data were obtained from nine different patches. Current amplitudes were normalized to 55 μM. The continuous line is a hyperbola with $K_m = 4.1$ μM. (*B*) Ca^{2+} dependence of the stationary inward current in the inward Na-Ca exchange mode generated by photolytic Ca^{2+} concentration jumps (Fig. 6). The continuous line is a hyperbola with $K_m = 4$ μM.

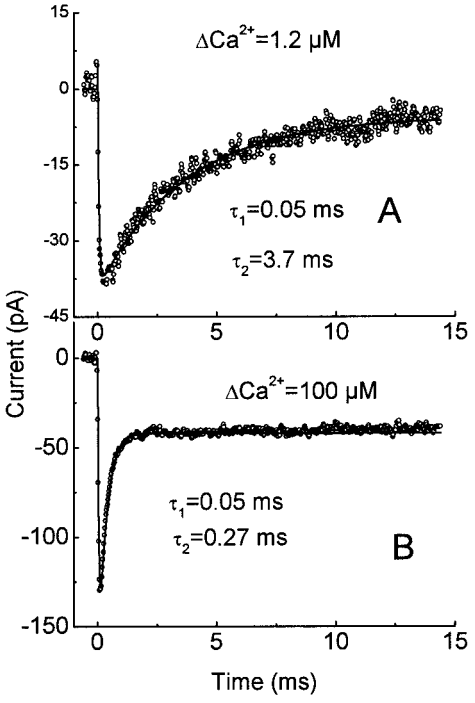

FIGURE 7 Current signals obtained in the inward Na-Ca exchange mode by Ca^{2+} concentration jumps of different magnitudes ($\Delta Ca^{2+} = 1.2$ and 100 μM). Holding potential is 0 mV. Both signals were fitted by a sum of two exponential functions.

the bath with different calibrated Ca^{2+} solutions (Table 1 in Kappl and Hartung, 1996b) or by the photolytic release of Ca^{2+}. The experiments provided an additional test to determine the magnitude of the Ca^{2+} concentration jump by comparison with the stationary currents obtained under both conditions. The experiments were performed under "zero-trans" conditions (Läuger 1987, i.e., Na_{ex} = 100 mM, Na_{in} = "0," Ca_{ex} = "0," Ca_{in} = variable), making Na^+ and Ca^{2+} translocation irreversible.

Fig. 6 *A* shows the Ca^{2+} concentration dependence of the stationary inward current obtained by bath application of different Ca^{2+} concentrations at 0 mV. Data were obtained from guinea pig myocytes. The currents are normalized to the current at 55 μM which was between 22 and 31 pA. The concentration dependence can be described by a Michaelis-Menten equation with an apparent affinity $K_m = 4.1 \pm 0.2$ μM (nine membrane patches). An apparent K_m of ~4 μM was also obtained by the photolytic release of Ca^{2+} (Fig. 6 *B*). This is comparable with a $K_m = 2.7$ μM obtained by Matsuoka and Hilgemann (1992) with Na_{ex} = 80 mM. In membrane patches excised from rat heart muscle cells we obtained a lower Ca^{2+} affinity: $K_m = 9.8 \pm 0.7$ μM (13 membrane patches, data not shown).

Ca^{2+} concentration dependence of the pre–steady-state inward current in the Na-Ca exchange mode

Fig. 7 shows current records obtained by a small (Fig. 7 *A*) and a large (Fig. 7 *B*) Ca^{2+} concentration jump (ΔCa^{2+} = 1.2 and 100 μM) from the same membrane patch under conditions which promote Na-Ca exchange current. The extracellular Na^+ concentration was 100 mM in these experiments. As under Ca-Ca exchange conditions, the rise-time is not significantly reduced at the lower Ca^{2+} concentration jump, whereas the peak and the plateau current, as well as the decay time constant, are significantly changed. Fig. 8 *A* shows the Ca^{2+} dependence of the peak current. The Ca^{2+} dependence of the decay rate constant $1/\tau_{2,Na\text{-}Ca}$ is displayed in Fig. 8 *B*. As outlined previously, the Ca^{2+} dependence of both parameters is distorted by the formation of Ca^{2+} spikes if the fraction of DM-nitrophen photolyzed is small. Again, it is important to note that the peak current as well as the relaxation rate constant saturate at $\Delta Ca^{2+} > 10$ μM.

Voltage-dependence of the stationary inward Na-Ca exchange current

The voltage dependence of the inward Na-Ca exchange current was measured by different protocols. During the

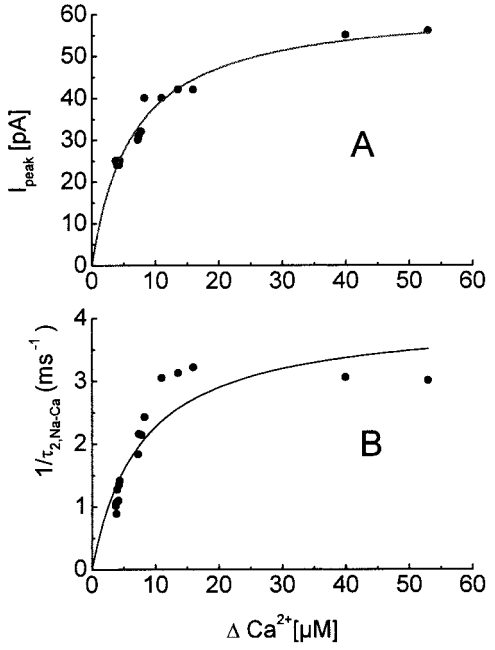

FIGURE 8 (*A*) Ca^{2+} dependence of the peak-inward current in Na-Ca exchange mode. The continous line is a hyperbola with $K_m = 6.4$ μM. Holding potential is 0 mV. (*B*) Ca^{2+} dependence of the relaxation of the peak current in the Na-Ca exchange mode

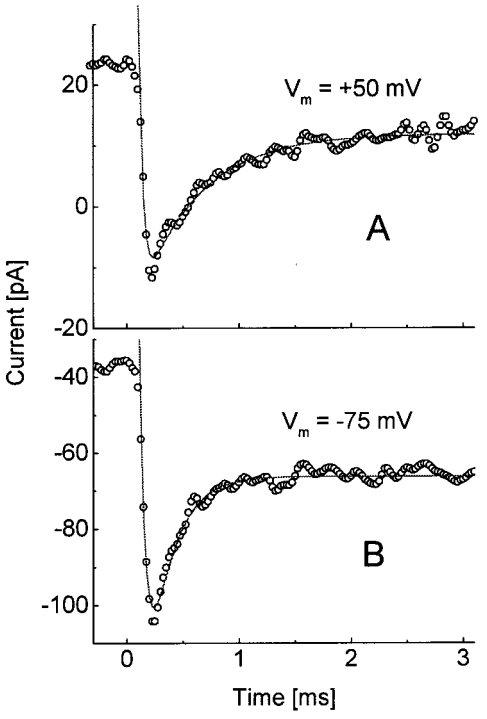

FIGURE 10 Current signals obtained in the inward Na-Ca exchange mode by Ca^{2+} concentration jumps ($\Delta Ca^{2+} = 7$ μM) at +50 and −75 mV. Both signals were fitted by a sum of two exponential functions with relaxation rate constants for the decaying phase $1/\tau_{2,Na\text{-}Ca}$ 1815 and 4554 s^{-1}, respectively.

stationary application of a saturating Ca^{2+} concentration, the membrane potential was changed to different levels (stationary inward current) or a photolytic Ca^{2+} concentration jump was performed at different levels of the membrane potential (pre–steady-state and stationary current).

Fig. 9 shows the voltage dependence of the stationary inward Na-Ca exchange current from seven different membrane patches from guinea pig myocytes. Na-Ca exchange current was obtained by applying identical voltage steps before and during the application of cytoplasmic Ca^{2+} (0.45 mM) and subtracting corresponding current records. The current voltage relations are normalized to 0 mV membrane potential. The figure contains I-V curves obtained from patches before and after the application of chymotrypsin. The slope of I-V curves was identical in both cases. Thus, deregulation seems not to affect the voltage dependence of the stationary inward current.

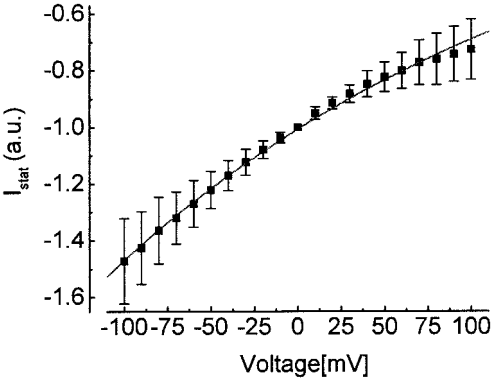

FIGURE 9 Voltage dependence of the stationary inward current in the Na-Ca exchange mode. Na-Ca exchange current was generated by applying 0.45 mM Ca^{2+} on the cytoplasmic side of the patch. The continuous line is fit of $I = I_o \cdot \exp(-V\alpha e_o/2kT)$ to the data with $\alpha = 0.19$.

The voltage dependence of inward Na-Ca exchange current in membrane patches from rat myocytes not treated with chymotrypsin is very similar to that in guinea pig cells.

Voltage dependence of pre–steady-state inward Na-Ca exchange current

Saturating Ca^{2+} concentration jumps were performed at different membrane potentials. All membrane patches were treated with chymotrypsin. Fig. 10 shows two current signals obtained at +50 mV and −75 mV after a Ca^{2+} concentration jump ($\Delta Ca = 100$ μM). It is evident that at +50 mV the amplitude of the peak current is smaller and the decay to the plateau is slower than at −75 mV. In addition, the steady-state current is reduced at positive voltages as expected from the stationary I-V curves described previously. Fig. 11 *A* shows the voltage dependence of the stationary current and of the peak current. The slope of the peak current is steeper than that of the stationary current.

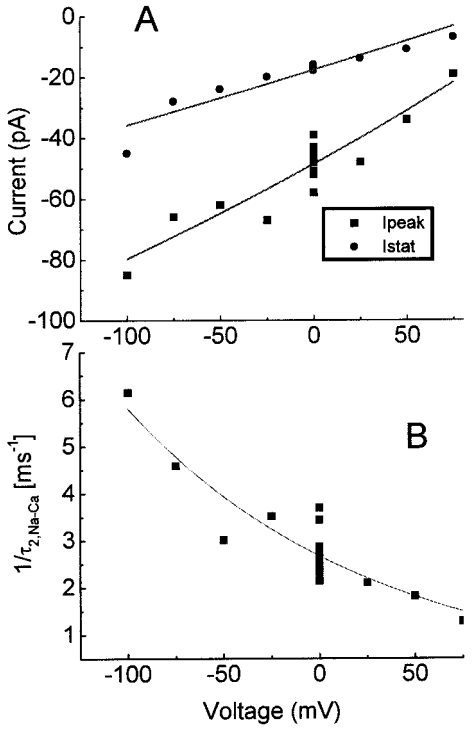

FIGURE 11 (*A*) Voltage dependence of the peak-current and the stationary current elicited by Ca^{2+} concentration jumps at different holding potentials. (*B*) Voltage dependence of the relaxation rate constant $1/\tau_{2,Na\text{-}Ca}$. The continuous line is fit of $1/\tau = 1/\tau_o \cdot \exp(-V\alpha e_o/2kT)$ to the data with $\alpha = 0.36$.

Fig. 11 *B* shows the voltage dependence of the decay rate constant $1/\tau_{2,Na\text{-}Ca}$ describing the decay of the peak current to the stationary current. The relaxation rate constant is reduced at positive voltages. The slope of the curve indicates that an apparent charge $\alpha = 0.36$ is associated with this relaxation (for details, see Fig. 11 *B*). A similar relation was obtained from two other membrane patches. It should be noted that under Ca-Ca exchange conditions, the relaxation rate constant is not voltage-dependent.

DISCUSSION

The results of the relaxation experiments described above are discussed in the framework of a consecutive reaction cycle (Läuger, 1987; Blaustein and Lederer, 1999) which implies that in the Na-Ca exchange mode, Na^+ and Ca^{2+} are translocated across the membrane sequentially and in separate reaction steps, whereas in the Ca-Ca exchange mode, the same pathway is used for inward and outward movement. Fig. 12 shows one possible version of such a reaction cycle. In the Na-Ca exchange mode with no Ca^{2+} outside and no Na^+ inside the transporter operates in a cyclic manner. In the Ca-Ca exchange mode the transporter shuttles reversibly between states E0 and E4 if Ca^{2+} is available on both sides of the membrane, implying that the

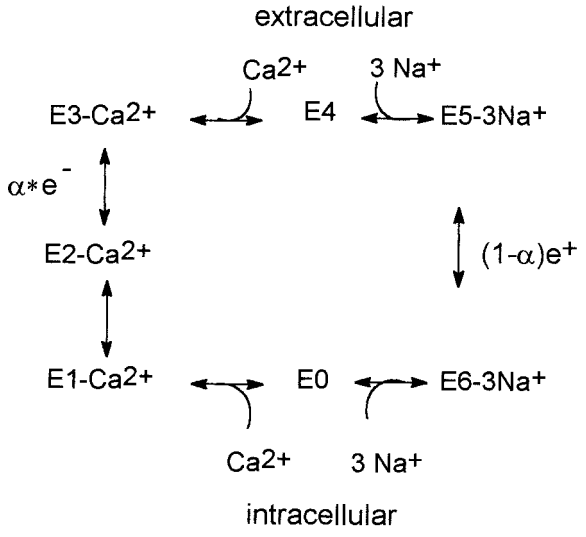

FIGURE 12 Reaction cycle of the Na-Ca exchanger. For simplicity it is assumed that 3 Na^+ bind in a single step to the extracellularly directed binding site E4. E0 is the intracellularly directed empty binding site. The Ca^{2+} translocating transition E2↔E3 and the Na^+ translocating transition E5↔E6 are assumed to be electrogenic. Ca^{2+} translocation is associated with the movement of negative net charge, and Na^+ translocation is associated with the movement of positive net charge.

transporter is in a true equilibrium. In the absence of Ca^{2+} on the cytoplasmic and high Ca^{2+} on the extracellular side, i.e., before the laser flash, most molecules will be in state E0. It is assumed that this condition is approximately fulfilled with a pre-flash Ca^{2+} concentration of <0.1 μM and an apparent Ca^{2+} affinity of ~ 4 μM. After a Ca^{2+} concentration jump the exchanger will reach another distribution of states which is again a dynamic equilibrium. The number of intermediates involved in Ca^{2+} translocation is derived from the experimental results as discussed below. Movement of net negative charge is assumed to be associated with the translocation of Ca^{2+}, and net positive charge is assigned to the translocation of Na^+ (Kappl and Hartung, 1996b).

A serious drawback of the photolabile Ca-chelators available at present is that Ca^{2+} concentration steps can be generated only within a narrow range of conditions, determined by the ratio of chelator and Ca^{2+} and the fraction of chelator photolyzed, whereas in most cases Ca^{2+} concentration spikes (Fig. 1) are generated because of rebinding of Ca^{2+} to nonphotolyzed, free chelator. This problem has been discussed first by Zucker (1993). In our previous study (Kappl and Hartung, 1996a, b), we avoided the formation of Ca^{2+} spikes by using solutions which contained total amounts of Ca^{2+} and chelator in a ratio close to 1 and high intensity laser light which photolyzed between 10 and 20% of total DM-nitrophen. Although the experiments reported here were also performed with solutions containing nearly equal amounts of Ca^{2+} and DM-nitrophen added, simulations show (see Fig. 1 and Material and Methods) that with

low flash intensities, i.e., small fractions of total DM-nitrophen–photolyzed (<10%) Ca^{2+} spikes are generated. Thus, one should be aware that the Ca^{2+} concentration step gradually mutates into a concentration spike if the energy of the laser flash is reduced. This means that the Ca^{2+} concentration is several times higher immediately after the flash than in equilibrium. These Ca^{2+} spikes distort the time course and the amplitude of the current signal considerably. The time to peak will be shortened and the peak amplitude will be increased whereas the decay rate may be slowed because it is determined by the slow rebinding of Ca^{2+} to DM-nitrophen (Fig. 1). However, the observation that the amplitude of the transient current and its relaxation rate are saturating functions of the Ca^{2+} concentration jump as well as the voltage and Ca^{2+} dependence of the charge translocation in the Ca-Ca exchange mode are not affected by Ca^{2+} spikes and provide important constraints on the minimal number of reaction steps and the assignment of electrogenicity to certain steps of the reaction cycle.

The results obtained in the Ca-Ca exchange mode are discussed first because fewer parameters are involved here and because a relaxation in this mode is a transition between two states of equilibrium rather than a transition from one stationary state to another, as in the Na-Ca exchange mode. The amount of charge translocated is an indicator for the equilibrium distribution of states established at different Ca^{2+} concentrations and voltages. In addition, the analysis of the partial reaction will help to understand the transport cycle in the Na-Ca exchange mode.

Ca-Ca exchange

The observation of an inward current elicited by a photolytic Ca^{2+} concentration jump on the cytoplasmic side strongly suggests that negative net charge is translocated by the exchanger loaded with Ca^{2+} (Hilgemann, 1996; Kappl and Hartung, 1996b). A transient inward current was also observed with oocyte membranes expressing Na-Ca exchanger from squid (He et al., 1998), indicating that this exchanger also translocates negative net charge together with Ca^{2+}.

A kinetic model describing the relaxation current in the Ca-Ca exchange mode should have the following properties: 1) the peak current and the relaxation rate constant $1/\tau_{2,Ca\text{-}Ca}$ saturate at large Ca^{2+} concentration jumps; 2) the amount of charge translocated is independent of the amount of Ca^{2+} released; 3) the amount of charge translocated is voltage-dependent; and 4) the relaxation rate constant $1/\tau_{2,Ca\text{-}Ca}$ is not voltage-dependent. The properties of Ca-Ca exchange enumerated above can be described by a four-step reaction (E0 to E4 in Fig. 12). For reasons discussed below, the intra- and extracellular Ca^{2+} binding reactions and the transition E1↔E2 are thought to be nonelectrogenic. Transition E1↔E2 is thought to be rate-limiting, whereas transition E2↔E3 is assumed to be fast-equilibrating and electrogenic.

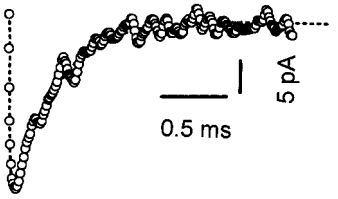

FIGURE 13 Fit of a set of differential equations (*dotted line*) describing the proposed model for Ca-Ca exchange (Fig. 12 and Appendix) to a current record (○) obtained after the release of 20 μM Ca^{2+} at 0 mV in the Ca-Ca exchange mode. The following numbers were assigned to rate constants by the fitting procedure: $k_{E0E1} = 2.8 \times 10^9\ M^{-1}s^{-1}$; $k_{E1E0} = 18{,}566\ s^{-1}$; $k_{E1E2} = 4330\ s^{-1}$; $k_{E2E1} = 50\ s^{-1}$. k_{E2E3} and k_{E3E2} were both set to 40,000 s^{-1}, and $k_{E3E4} = 2 \times 10^6\ s^{-1}$, $k_{E4E3} = 2 \times 10^9\ M^{-1}s^{-1}$. For details see Appendix.

The observation that the peak current and the relaxation rate constant saturate provides strong evidence that Ca^{2+}-binding at cytoplasmic binding sites is not electrogenic. With electrogenic Ca^{2+}-binding both parameters would increase in proportion to the magnitude of the Ca^{2+} concentration step without saturation (Fig. 13 and Appendix). It should be noted, however, that saturation could be introduced indirectly by the bandwidth of the recording system. But this limit (15 μs or 10 kHz) was not reached in these experiments.

Saturation can be obtained if the electrogenic transition itself or a transition preceding the electrogenic transition is rate-limiting for the relaxation. The possibility that the electrogenic transition itself is rate-limiting can be excluded because the observed relaxation rate constant $1/\tau_{2,Ca\text{-}Ca}$ is not voltage-dependent. It is assumed, therefore, that this relaxation is related to a slow electroneutral transition. Electrogenicity is assigned to at least one following transition which is equilibrating so fast that its time course cannot be observed. For simplicity, it is also assumed that this voltage-dependent transition (E2↔E3) accounts for the Ca^{2+} independence of the charge translocation, i.e., this step is predominant for the equilibrium distribution of states. Therefore, large forward and backward rate constants are assigned to this step (see Appendix) which imply that the equilibrium distribution of states is more or less independent of the cytoplasmic Ca^{2+} concentration. In Fig. 12 this electrogenic transition is a second conformational one followed by the external Ca^{2+} binding reaction. Thus, it is assumed that at least four transitions are involved in Ca^{2+} translocation. It should be noted that a three-step model would be sufficient if electrogenicity is assigned to external Ca^{2+} binding. This, however, does not seem reasonable because Matsuoka and Hilgemann (1992) have provided evidence that Ca^{2+} binding to external sites is not voltage-dependent. Furthermore, the experiments described here were performed with 5 mM extracellular Ca^{2+} which is at

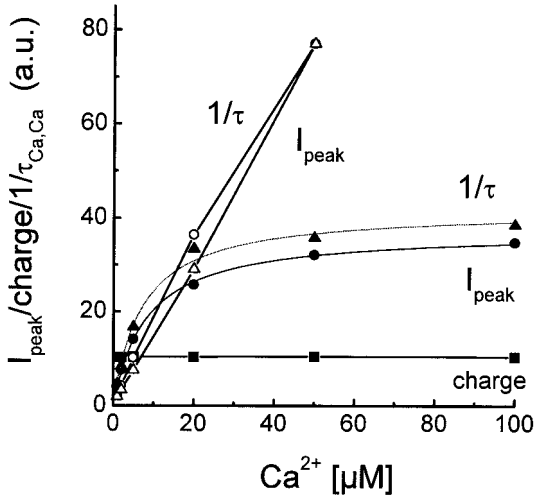

FIGURE 14 Simulation of the Ca^{2+} dependence of the peak current, the relaxation rate constant, and the charge translocation with the model proposed for Ca-Ca exchange (Fig. 12 and Appendix) and the rate constants given in figure legend 13 (for further details see Appendix). It is shown that the peak current (●) and the relaxation rate constant (▲) saturate with increasing Ca^{2+} concentration if electrogenicity is placed on the E2↔E3 transition, whereas the amount of charge translocated (■) is fairly independent from the amount of Ca^{2+} released. However, the peak current (△) and the relaxation rate constant (○) increase linearly if electrogenicity is placed on the binding reaction (E0↔E1).

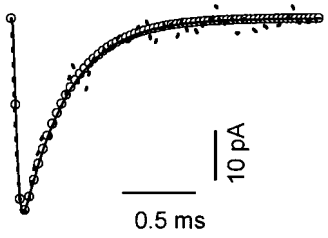

FIGURE 15 Current trace recorded at 0 mV (*dotted line*) in the Ca-Ca exchange mode. Superimposed are two simulated curves using the model from Fig. 12 and the kinetic contents in Fig. 13, but setting the voltage to +100 (○) and −100 mV (*solid line*). The voltage dependence of rate constants k_{E2E3} and k_{E3E2} is calculated by $k(V) = k(0)\exp(-\alpha \cdot V/53)$. An apparent charge $\alpha = 0.38$ is assumed (see Results). It is obvious that the time course is voltage-independent. The traces at 0 mV and +100 mV were scaled by factors of 1.6 and 4.2, respectively, to facilitate comparison of the time course.

least five times higher than the half-saturating concentration (Matsuoka and Hilgemann, 1992; Blaustein and Lederer, 1999). Thus, voltage-dependent Ca^{2+} binding is expected to be negligible at this concentration.

In conclusion, it is suggested that Ca-Ca exchange can be described by a four-state model with electroneutral binding of Ca^{2+} on both sides of the membrane and two conformational transitions. The first transition after Ca^{2+}-binding on the cytoplasmic side is electroneutral and rate-limiting, whereas the second conformational transition is fast and electrogenic. Matsuoka and Hilgemann (1992) have discussed three models to describe the voltage and substrate dependence of inward and outward exchange current. A common property of these models is that Ca^{2+} translocation occurs in five reaction steps: two binding reactions and three conformational transitions. This is one more conformational transition than in our model. At present, we have no experimental evidence for including an additional reaction step, e.g., between extracellular Ca^{2+} binding and the electrogenic transition which would not change the interpretation of our results.

The Ca^{2+} concentration dependence of the model has been simulated (for details, see Appendix). The results of these simulations are summarized in Figs. 13–15. The suggested model is compatible with the experimental results: the relaxation rate constant and the peak current saturate with increasing Ca^{2+} concentrations and the charge translocation is fairly independent from the magnitude of the Ca^{2+} concentration jump. For comparison we have also included the Ca^{2+} dependence of the peak current and the relaxation rate constant which is obtained if Ca^{2+} binding is made electrogenic. Both parameters increase linearly with Ca^{2+}.

Relaxation experiments with voltage (Hilgemann, 1996) and Ca^{2+} concentration jumps (Kappl and Hartung, 1996a, b) show that individual transitions of Ca-Ca exchange are electrogenic. In the Ca-Ca exchange mode, voltage jumps induce an outward movement of charge at depolarizing and an inward current at hyperpolarizing potentials. This agrees with the idea, derived from Ca^{2+} concentration jumps, that the Ca^{2+}-loaded cardiac exchanger carries negative charge (Hilgemann, 1996; Kappl and Hartung, 1996b). In contrast, the amount of charge translocated after a Ca^{2+} concentration jump is smaller at positive than at negative potentials, indicating that less binding sites are oriented toward the extracellular side at positive potentials than at negative potentials. Within the framework of the reaction cycle this could be reached by increasing or reducing the appropriate voltage-dependent rate constants of the E2↔E3 transition. We suggest that the backward reaction shifting charge toward the cytoplasmic side (E3→E2) is accelerated because this would agree with the observation that relaxations induced by a voltage jump are accelerated at positive potentials (Hilgemann, 1996). Acceleration of a backward reaction could also explain the reduction of ^{45}Ca efflux at positive potential observed in squid axon (DiPolo and Beaugé, 1987).

Our assignment of electrogenicity to the E2↔E3 transition contradicts a previous suggestion by Matsuoka and Hilgemann (1992) who suggested that occlusion on the cytoplasmic side, i.e., the E1↔E2 transition should be electrogenic. whereas occlusion on the extracellular side should be nonelectrogenic. According to the discussion outlined previously, this assignment is not compatible with our results because a voltage-dependent relaxation rate constant should be observed.

It should be noted, however, that Hilgemann et al. (1991) investigated the voltage and Ca^{2+} dependence of inward and outward Na-Ca exchange current and not Ca-Ca exchange. Thus, under their conditions at least two voltage-dependent transport steps, i.e., Na^+ and Ca^{2+} translocation, contribute to the current voltage relation. The lowest cytoplasmic Ca^{2+} concentration used by Matsuoka and Hilgemann (1992) was 1 μM, which has to be compared with an affinity of 4 μM. We suggest that the voltage dependence of inward Na-Ca exchange at this concentration is maintained because Na^+ translocation is rate-limiting. Furthermore, the voltage dependence of inward exchange current at low cytoplasmic Ca^{2+} seems to depend critically on the experimental conditions. In contrast to Matsuoka and Hilgemann (1992), Hilgemann et al. (1991) claimed that voltage dependence disappears at low cytoplasmic Ca^{2+} and suggested electrically silent Ca^{2+} translocation.

Na-Ca exchange mode

In the Na-Ca exchange mode a Ca^{2+} concentration jump does not establish a new equilibrium as in the Ca-Ca exchange mode; rather, it induces a relaxation to a new stationary state which is determined by the complete reaction cycle which translocates 1 Ca^{2+} outward and 3 Na^+ inward. The release of Ca^{2+} on the extracellular side and the release of Na^+ on the cytoplasmic side are irreversible because of the "zero-trans" conditions. Under these conditions a Ca^{2+} concentration jump elicits a transient current declining to a stationary current. The transient current observed in the Na-Ca exchange mode shares many properties with the transient observed in the Ca-Ca exchange mode. The most significant difference known so far is the voltage dependence of the decay rate constant in the Na-Ca exchange mode.

Stationary current

Stationary current voltage relations of the inward Na-Ca exchange current have been determined before with the whole-cell mode of the patch-clamp technique (Kimura et al., 1986; Niggli and Lederer, 1991, 1993; Powell et al., 1993) and with giant excised membrane patches (Matsuoka and Hilgemann, 1992; Hilgemann 1996). The inward current increases at negative potentials, indicating a higher turnover number. Although the increment of the peak current indicates that Ca^{2+} translocation is accelerated by negative potentials (see Ca-Ca exchange), we suggest that the increment of the stationary inward current is mainly attributable to the acceleration of the Na^+ translocating branch of the reaction cycle because Na^+ translocation is rate-limiting in the Na-Ca exchange mode (Kappl and Hartung, 1996b).

Pre–steady-state current

The pre–steady-state current generated by a Ca^{2+} concentration jump in the Na-Ca exchange mode shares many features with the transient current observed in the Ca-Ca exchange mode. In both modes the peak current and the decay rate constant saturate with increasing Ca^{2+} concentrations. This is not surprising because the transport process is started by the same reaction steps in both modes, i.e., by Ca-binding and translocation. A major difference concerns the voltage dependence of the decay rate constant. This relaxation is voltage-independent in the Ca-Ca exchange mode, but voltage-dependent in the Na-Ca exchange mode in which it increases at negative voltages. This could indicate that in the Na-Ca exchange mode, the Na^+ translocating branch of the reaction cycle contributes to the relaxation to the steady-state. In contrast, it has been shown that the relaxation rate constant is smaller in the Na-Ca exchange mode than in the Ca-Ca exchange mode (Kappl and Hartung, 1996b). Thus, it seems reasonable to assume that in the Na-Ca exchange mode the Na^+ translocating branch of the cycle contributes to the relaxation rate constant $1/\tau_{2,\text{Na-Ca}}$.

CONCLUSION

The experiments reported here provide evidence that Ca^{2+}-binding on the cytoplasmic side is not electrogenic. At least two conformational transitions are involved in Ca^{2+} translocation. One of them is voltage-independent and rate-limiting for Ca-Ca exchange, whereas the other is electrogenic and fast. In the Na-Ca exchange mode the Na^+ translocating branch seems to contribute to the relaxation induced by a Ca^{2+} concentration jump, but it seems difficult to separate both reactions.

The authors thank Doris Ollig and Dagmar Stiegert for isolating myocytes, Prof. E. Bamberg for continuous support, Dr. C. Grewer for discussions, and Prof. M. Blaustein for reading the manuscript.

APPENDIX

Simulations of the experiments in the Ca-Ca exchange mode were performed on the basis of the reaction cycle shown in Fig. 12. The reaction steps involved in Ca-Ca exchange are shown below:

$$Ca^{2+} + E0 \leftrightarrow E1 \leftrightarrow E2 \leftrightarrow E3 \leftrightarrow E4 + Ca^{2+}$$

with rate constants: k_{E0E1}, k_{E1E0}, k_{E1E2}, k_{E2E1}, k_{E2E3}, k_{E3E2}, k_{E3E4}, k_{E4E3}.

A set of simultaneous differential equations describing this reaction was integrated numerically (Scientist software). An initial set of data for the rate constants was obtained by fitting the set of differential equations to a current record obtained experimentally (Fig. 13). The rate of release of Ca^{2+} from DM-nitrophen is limited to 38,000 s^{-1} (Ellis-Davies et al., 1996). The rate constants for the E2↔E3 were forced to be larger than that of the E1↔E2 transition. Extracellular Ca^{2+} was fixed to 5 mM, and the Ca^{2+} concentration jump was 20 μM. The rate constants obtained by the fit are listed in the legend of Fig. 13. It can be seen that a relatively large

association rate constant ($>2 \times 10^9$ $M^{-1}s^{-1}$) for Ca^{2+} on the cytoplasmic side is obtained. This is required to obtain the time to peak of ~0.1 ms at Ca^{2+} concentrations of ~20 μM. For the simulations we have used 2×10^9 $M^{-1}s^{-1}$ for the association rate constant on both sides. The same association rate constant is assumed for extracellular Ca^{2+} binding. A somewhat lower association rate constant is sufficient, if faster release of Ca^{2+} is assumed. But even if the Ca^{2+} release occurs with 10^5 s^{-1} the association rate has to be $\sim 1 \times 10^9$ $M^{-1}s^{-1}$.

The dissociation rate constant on the cytoplasmic side is set to 8000 s^{-1} to account for the Ca^{2+} affinity of 4 μM (see Results). The dissociation rate constant on the extracellular side is set to 2×10^6 s^{-1} to account for the extracellular Ca^{2+} affinity of 1 mM (Blaustein and Lederer, 1999). The forward and backward rate constants for the E2↔E3 transition in the absence of an applied voltage are both set to 40,000 s^{-1}. The magnitude of these rate constants is set much higher than that of the E1↔E2 transition to account for the observation that no voltage-dependent relaxation rate is observed and for the Ca^{2+} independence of the charge translocation (Fig. 3).

The rate constants for the E1↔E2 transition were taken from the original fit (see legend of Fig. 13) 4330 s^{-1} and 50 s^{-1}, respectively. To simulate the Ca^{2+} concentration dependence, the system of differential equations was integrated with Scientist software at different Ca^{2+} concentrations. The resulting curves were then fitted with two exponential functions to obtain the relaxation rate constant and integrated to determine the charge translocation.

In a first set of simulations electrogenicity was assigned to the E2↔E3 transition.

Fig. 14 shows that, in accordance with experimental observation, the peak current and the relaxation rate saturate if electrogenicity is assigned to this transition. Furthermore, the relaxation time constant is voltage-independent under this condition (Fig. 15). Fig. 14 also shows the Ca^{2+} dependence of the peak current and the relaxation rate constant obtained if electrogenicity is placed on Ca^{2+} binding (E0↔E1). The peak current and the relaxation rate constant are linearly dependent on the magnitude of the Ca^{2+} concentration jump.

REFERENCES

Bartschat, D. K., and G. E. Lindenmayer. 1980. Calcium movements promoted by vesicles in a highly enriched sarcolemma preparation from canine ventricle. Calcium-calcium countertransport. *J. Biol. Chem.* 255: 9626–9634.

Blaustein, M. P., and W. J. Lederer. 1999. Sodium/calcium exchange: Its physiological implications. *Phys. Rev.* 79:763–854.

Blaustein, M. P., and J. M. Russell. 1975. Sodium-calcium exchange and calcium-calcium exchange in internally dialyzed squid giant axons. *J. Membr. Biol.* 22:285–312.

DiPolo, R., and L. Beaugé. 1987. Characterization of the reverse Na/Ca exchange in squid axons and its modulation by Ca and ATP. Ca_i-dependent Na_i/Ca_o and Na_i/Na_o exchange. *J. Gen. Physiol.* 90:505–525.

DiPolo, R., and L. Beaugé. 1990. Asymmetrical properties of the Na-Ca exchanger in voltage-clamped, internally dialyzed squid axons under symmetrical ionic conditions. *J. Gen. Physiol.* 95:819–835.

Ellis-Davies, G. C., J. H. Kaplan, and R. J. Barsotti. 1996. Laser photolysis of caged calcium: rates of calcium release by nitrophenyl-EGTA and DM-nitrophen. *Biophys. J.* 70:1006–1016.

He, Z., Q. Tong, B. T. Quedneau, K. D. Philipson, and D. W. Hilgemann. 1998. Cloning, expression, and characterization of the squid Na^+-Ca^{2+}exchanger (NCX-SQ1). *J. Gen. Physiol.* 111:857–873.

Hilgemann, D. W. 1989. Giant excised cardiac sacrolemmal membrane patches: sodium and sodium-calcium exchange currents. *Pflügers Arch.* 415:247–249.

Hilgemann, D. W. 1990. Regulation and deregulation of cardiac Na^+-Ca^{2+} exchange in giant excised sarcolemmal membrane patches. *Nature.* 344:242–245.

Hilgemann, D. W. 1996. Unitary cardiac Na^+, Ca^{2+} exchange current magnitudes determined from channel-like noise and charge movements of ion transport. *Biophys. J.* 71:759–768.

Hilgemann, D. W., D. A. Nicoll, and K. D. Philipson. 1991. Charge movement during Na^+ translocation by native and cloned cardiac Na^+/Ca^{2+} exchanger. *Nature.* 352:715–718.

Kaplan, J., and G. C. R. Ellis-Davies. 1988. Photolabile chelators for the rapid photorelease of divalent cations. *Proc. Natl. Acad. Sci. U.S.A.* 85:6571–6575.

Kappl, M., and K. Hartung. 1996a. Kinetics of Na-Ca exchange current after a Ca^{2+} concentration jump. *In* D. W. Hilgemann, K. D. Philipson, and G. Vassort editors. Sodium-Calcium Exchange: Proceedings of the Third International Conference. New York, Academy of Science.

Kappl, M., and K. Hartung. 1996b. Rapid charge translocation by the Na+-Ca^{2+} exchanger after a Ca^{2+} concentration jump. *Biophys. J.* 71:2473–2485.

Kimura, J., A. Noma, and H. Irisawa. 1986. Na-Ca exchange current in mammalian heart cells. *Nature.* 319:596–597.

Läuger, P. 1987. Voltage dependence of sodium-calcium exchange: predictions from kinetic models. *J. Membr. Biol.* 99:1–11.

Matsuoka, S., and D. W. Hilgemann. 1992. Steady-state and dynamic properties of cardiac sodium-calcium exchange: ion and voltage dependencies of the transport cycle. *J. Gen. Physiol.* 100:963–1001.

McCray, J. A., N. Fidler-Lim, G. C. Ellis-Davies, and J. H. Kaplan. 1992. Rate of release of Ca^{2+} following laser photolysis of the DM-nitrophen-Ca^{2+} complex. *Biochemistry.* 31:8856–8861.

Mechmann, S., and L. Pott. 1986. Identification of Na-Ca exchange current in single cardiac myocytes. *Nature.* 319:597–599.

Niggli, E., and W. J. Lederer. 1991. Molecular operations of the sodium-calcium exchanger revealed by conformation currents. *Nature.* 349: 621–624.

Niggli, E., and W. J. Lederer. 1993. Activation of Na-Ca exchange current by photolysis of "caged calcium." *Biophys. J.* 65:882–891.

Powell, T., A. Noma, T. Shioya, and R. Z. Kozlowski. 1993. Turnover rate of the cardiac Na^+-Ca^{2+} exchanger in guinea-pig ventricular myocytes. *J. Physiol.* 472:45–53.

Slaughter, R. S., J. L. Sutko, and J. P. Reeves. 1983. Equilibrium calcium-calcium exchange in cardiac sarcolemmal vesicles. *J. Biol. Chem.* 258: 3183–3190.

Zucker, R. S. 1993. The calcium concentration clamp: spikes and reversible pulses using the photolabile chelator DM-nitrophen. *Cell Calcium.* 14:87–100.